

Iris recognition algorithm based on point covering of high-dimensional space and neural network

Wenming Cao^{1,2}, Jianhui Hu¹, Gang Xiao¹, Shoujue Wang²

¹The College of Information Engineering, ZheJiang University of Technology,
Hangzhou, 310014, China

²Lab of Artificial Neural Networks, Institute of Semiconductors, CAS, Beijing, 100083,
China
csann@zjut.edu.cn

Abstract. In this paper, we constructed a neuron of point covering of high-dimensional space, and proposed a new method for iris recognition based on point covering theory of high-dimensional space. In this method, irises are trained as “cognition” one class by one class, and it doesn’t influence the original recognition knowledge for samples of the new added class. The results of experiments show the rejection rate is 98.9%, the correct cognition rate and the error rate are 95.71% and 3.5% respectively. The experimental results demonstrate that the rejection rate of test samples excluded in the training samples class is very high. It proves the proposed method for iris recognition is efficacy.

1. Introduction

In recent years, with the development of information technology and the increasing need for security, intelligent personal identification has become a very important and urgent problem. The emerging biometric technology can solve the problem, which takes the unique, reliable and stable biometric features (such as fingerprints, iris, face, palm-prints, gait etc.) as identification body. This technology has very high security, reliability and effectivity. As one of the biometric technology, iris recognition has very high reliability. Comparing with other biometric identification technology, the fault acceptance rate and the fault rejection rate of iris recognition are very low. The technology of iris recognition has many advantages, i.e., stability, non-invasiveness, uniqueness. All these desirable properties make the technology of iris recognition has very high commercial value. Based on the above reasons, many researchers have applied themselves to this field. Daugman used multi-scale quadrature wavelets to extract texture-phase structure information of iris to generate a 2048-bit iriscode and compared the difference between a pair of iris representations by computing their Hamming distance via the XOR operator [1],[2]. Wildes et al. represented the iris texture with a Laplacian pyramid constructed with four different resolution levels and used the normalized correlation to determine whether the input image and the model image are from the same class [3]. Boles et al. calculated zero-crossing representation of 1D wavelet transform at various resolution levels of a virtual circle on an iris image

to characterize the texture of the iris. Iris mating was based on two dissimilarity functions [4][10][11]. In this paper, from the cognition science point of view, we constructed a neuron of point covering of high-dimensional space[5][6][7], and propose a new method for iris recognition based on point covering theory of high-dimensional space and neural network[8][12]. The results of experiments show the rejection rate is 98.9%, the correct recognition rate and the error rate are 95.71% and 3.5% respectively. The experimental results demonstrate that the rejection rate of test samples excluded in the training samples class is very high. It proves the proposed method for iris recognition is effective.

The remainder of this paper is organized as follows. Section 2 describes image preprocessing. Section 3 introduces iris recognition algorithm based on point covering theory of multi-dimensional space and neural network. Experiments results and experimental analysis are given in Section 4 and Section 5 respectively.

2. Image preprocessing

Iris image preprocessing is mainly composed of iris localization, iris normalization and enhancement.

2.1 Iris localization

Iris localization namely is the localization of the inner boundary and the outer boundary of a typical iris can approximately be taken as circles. It is the important part of the system of iris recognition, and exact localization is the premise of the iris identification and verification.

2.1.1 Localization of the inner boundary

The original iris image (see Fig.1(a)) has some character of the gray-scale distribution. The iris is darker than the sclera, and the pupil is greatly darker than the iris, as shown in Fig.1(a). From the histogram (see Fig.1(b)), we can clearly see that the low gray-scale mainly converges at the first peak value. Therefore, we adopt the binary transform to localize the inner boundary. From the image after binary transform (see Fig.2(a)), we find that the areas of zero gray-scale are almost the areas of the pupil and eyelash. Therefore, we reduce the influence of the eyelash by erode and dilation (see Fig.2(a)).

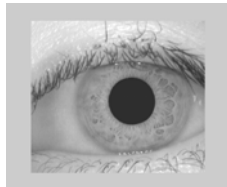
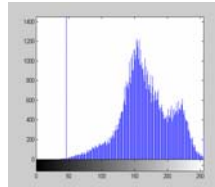


Fig.1 (a) original image



(b) histogram of the iris

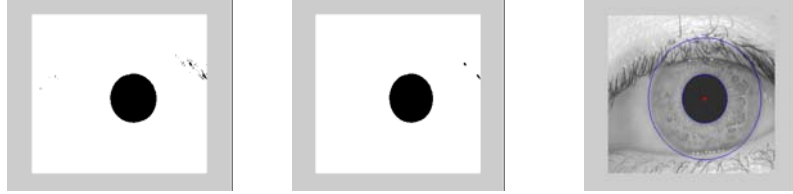


Fig.2(a) binary image (b) binary image after erode and dilation (c) localized image

From the Fig 2(b), we can find that the length and the midpoint of the longest chord can be taken as the approximate diameter and center of the pupil respectively. Namely, according the geometry knowledge, let the length of the longest chord is $dia\ max$, and the coordinates of the first point of the chord are $xbegin$ and $ybegin$, then

$$xpupil = xbegin + \frac{dia\ max}{2}, ypupil = ybegin, rpupil = \frac{dia\ max}{2} \quad (1)$$

Where $xpupil$ and $ypupil$ denote the center coordinates of the pupil, and $rpupil$ denotes the radius of the pupil.

When the quality of the image is reliable, this algorithm can localize the pupil quickly and exactly. Otherwise, we can correct the method as follow:

1. We can reduce the searching area by subtracting the pixels on the edge of the image.
2. We can get k chords, which are less than a certain threshold near the longest chord, and take the average value of center coordinates of k chord as the center of the pupil.

2.1.2 Localization of the outer boundary

The exact parameters of the outer boundary are obtained by using edge detection (Canny operator in our experiments) and Hough transform. The image after Edge detection includes some useless points. For eliminating the influence, we remove the useless points between the areas of $[30^\circ, 150^\circ]$ and $[225^\circ, 315^\circ]$ according to the center of the pupil. Then, Hough transform is adopted to localize the outer boundary.

By the above method, we can localize the inner boundary and the outer boundary of the iris exactly. The localizations results of the iris are showed in Fig.2(c).

2.2 Iris normalization and enhancement

Iris from different people may be captured in different size, and even for irises from the same eye, the size may change because of illumination variations and other factors (the pupil is very sensitive to lighting changes). Such elastic deformation in iris texture will influence the results of iris recognition. For the purpose of achieving more accurate recognition results, it is necessary to compensate for such deformation.

In our experiment, every point of the iris image is mapped to the polar coordinates by the following formula.

$$\begin{cases} x(r, \theta) = (1-r)x_p(\theta) + rx_s(\theta) \\ y(r, \theta) = (1-r)y_p(\theta) + ry_s(\theta) \end{cases} \quad (2)$$

In which, $(x_p(\theta), y_p(\theta))$ and $(x_s(\theta), y_s(\theta))$ denote the point of intersection with the inner boundary and the outer boundary respectively.

In our experiment, the sector areas $([130^\circ, 230^\circ])$ and $([310^\circ, 410^\circ])$ are intercepted for normalization according the pupil center. In this way, one hand, it is simple; on the other hand, the segment texture information is enough to identify the different persons. Then, the iris ring is unwrapped to a rectangular texture block with a fixed size (64×256) , and the rows correspond to the radius and the columns correspond to the angles (see Fig.3(a)). The normalized iris image still has low contrast and may have non-uniform brightness caused by the position of light sources. All these may affect the feature analysis. Therefore, we enhance the normalized image by means of histogram equalization. Such processing compensates for non-uniform illumination, as well as improving the contrast of the image. The enhanced image is shown in Fig.3(b).

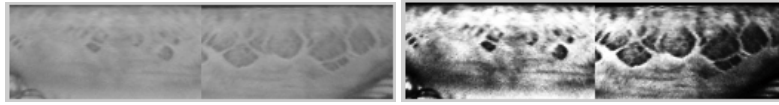


Fig.3(a) normalized image (b)enhanced image

3. Iris recognition algorithm based on point covering of multi-dimensional space and neural network

Multi-weighted neuron can be represented as following formula:

$$Y = f[\Phi(X, W_1, W_2, \dots, W_m) - Th] \quad (3)$$

In which, $\Phi(X, W_1, W_2, \dots, W_m)$ denotes the relation between the input point X and m weight (W_1, W_2, \dots, W_m) . Let $m = 3$, it is 3-weighted neuron, named $pSi3$. And $pSi3$ can be described as follow:

$$Y = f[\Phi(X, W_1, W_2, W_3) - Th] \quad (4)$$

$$\Phi(X, W_1, W_2, W_3) = \|X - \theta_{(W_1, W_2, W_3)}\| \quad (5)$$

In which, $\theta_{(W_1, W_2, W_3)}$ denotes the finite area, which is enclosed by three points(W_1 、 W_2 、 W_3), and it is a triangle area. Namely, $\theta_{(W_1, W_2, W_3)}$ can be represented as follow:

$$\theta_{(W_1, W_2, W_3)} = \{Y | Y = \alpha_1 W_1 + (1 - \alpha_1) W_2 + (1 - \alpha_2) W_3, \alpha_1 \in [0, 1], \alpha_2 \in [0, 1]\} \quad (6)$$

Then, $\Phi(X, W_1, W_2, W_3) - Th$ actually is the Euclid distance from X to the triangle area of the $pSi3$ neuron. The model of activation function is:

$$f(x) = \begin{cases} 1, & x \leq Th \\ -1, & x > Th \end{cases} \quad (7)$$

In multi-dimensional space, we use every three sample's points of the same class to construct a finite 2D plane, namely, a triangle. Then several 2D spaces can be constructed, and we cover these planes by the $pSi3$ neuron to approximate the complicated "shape", which is formed by many sample points of the iris in multi-dimensional space.

3.1 Construction of point covering area of multi-dimensional space

Step 1: Let the sample points of the training set are $\alpha = \{A_1, A_2, \dots, A_N\}$. In which, N is the number of the total sample points. To figure out the distance of every two points, the two points having the least distance are defined as B_{11} and B_{12} . Let B_{13} denotes the nearest point away from B_{11} and B_{12} , and B_{13} must doesn't in the line formed by B_{11} and B_{12} . In this way, B_{11} 、 B_{12} and B_{13} construct the first triangle plane represented as θ_1 , which is covered by a $pSi3$ neuron, the covering area is:

$$P_1 = \{X | \rho_{X\theta_1} \leq Th, X \in R^n\} \quad (8)$$

$$\theta_1 = \{Y | Y = \alpha_1 B_{11} + (1 - \alpha_1) B_{12} + (1 - \alpha_2) B_{13}, \alpha_1 \in [0, 1], \alpha_2 \in [0, 1]\} \quad (9)$$

Where $\rho_{X\theta_1}$ denotes the distance from X to θ_1 .

Step 2: Firstly, The rest points contained in P_1 should be removed. Then, according to the method of step1, define the nearest point away from B_{11} , B_{12} and B_{13} as B_{21} . Among B_{11} , B_{12} and B_{13} , two nearest points away from B_{21} are denoted as B_{22} and B_{23} . And B_{21} , B_{22} and B_{23} construct the second triangle defined as θ_2 , which is covered by another *pSi3* neuron. And the covering area is described as follow:

$$P_2 = \{X \mid \rho_{X\theta_2} \leq Th, X \in R^n\} \quad (10)$$

$$\theta_2 = \{Y \mid Y = \alpha_1 B_{21} + (1 - \alpha_1) B_{22} + (1 - \alpha_2) B_{23}, \alpha_1 \in [0,1], \alpha_2 \in [0,1]\} \quad (11)$$

Where $\rho_{X\theta_2}$ denotes the distance from X to θ_2 .

Step 3: Remove the rest points contained in the covering area of the front $(i-1)$ *pSi3* neurons. Let B_{i1} denotes the nearest point from the remained points to the three vertexes of the $(i-1)th$ triangle. Two nearest vertexes of the $(i-1)$ triangle away from B_{i1} are represented as B_{i2} and B_{i3} . Then, B_{i1} , B_{i2} and B_{i3} construct the i th triangle, defined as θ_3 .

In the same way, θ_3 is covered by a *pSi3* neuron. The covering area is

$$P_i = \{X \mid \rho_{X\theta_i} \leq Th, X \in R^n\} \quad (12)$$

$$\theta_3 = \{Y \mid Y = \alpha_1 B_{i1} + (1 - \alpha_1) B_{i2} + (1 - \alpha_2) B_{i3}, \alpha_1 \in [0,1], \alpha_2 \in [0,1]\} \quad (13)$$

Step 4: Repeat the step 3 until all sample points are conducted successfully. Finally, there are m *pSi3* neurons, and their merge about covering area is the covering area of every iris' class.

$$P = \bigcup_{i=1}^m P_i \quad (14)$$

3.2 Iris recognition algorithm based on point covering of high-dimensional space

Taking $Th=0$ under recognition, the *pSi3* neuron can be described as follow:

$$\rho = \left\| X - \theta_{(w_1, w_2, w_3)} \right\| \quad (15)$$

The output ρ is the distance from X to the finite area $\theta_{(w_1, w_2, w_3)}$.
The distance from X to the covering area of the i th class iris is:

$$\rho_i = \min_{j=1}^{M_i} \rho_{ij}, \quad i = 1, \dots, 80 \quad (16)$$

In which, M_i denotes the number of the $pSi3$ neuron of the i th iris, ρ is the distance from X to the covering area of the j th neuron of the i th class' iris.

The X will be classified to the iris class corresponding to the least ρ_i . Namely, the classification method is:

$$j = \min_{i=1}^{80} \rho_i, \quad j \in (1, \dots, 80) \quad (17)$$

4. Experimental results

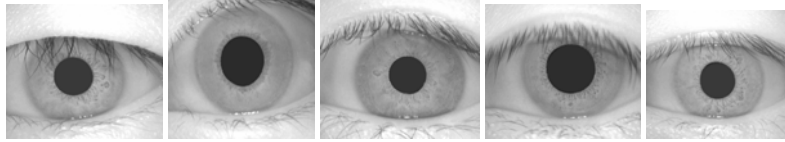


Fig.4 iris samples from the training set

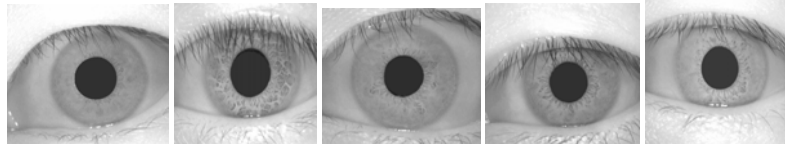


Fig.5 iris samples from the second test set

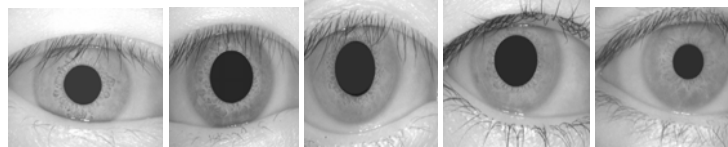


Fig.6 iris samples from the first test set

Images of CASIA (Institute of Automation, Chinese Academy of Sciences) iris image database are used in this paper. The database includes 742 iris images from 106 different eyes (hence 106 different classes) of 80 subjects. For each iris class, images

are captured in two different sessions and the interval between two sessions is one month. The experiment processes and experiment results are presented as follow:

(1) In our experiment, 3 random samples from each class in the frontal 80 classes (hence, 240 samples) are chosen for training, and a $pSi3$ neuron of multi-weighted neural network is constructed for the 3 samples. Five samples from the training set are shown in Fig.4. Then, the entire iris database is taken as test sample set. In which, 182 (26×7) samples, which don't belong to the classes of training samples, are referred to the first sample set. The remainder of total 560 (80×7) samples is referred to the second sample set. Fig.5 shows five samples from the second test set and Fig.6 shows five samples from the first test set.

(2) The rejection rate = the number of samples which are rejected correctly in the first sample set / the total number of the first sample set. The correct cognition rate = the number of samples which are recognized corrected in the second sample set / the total number of the second sample set. The error recognition rate = (the number of samples which are recognized mistakenly in the first sample set + the number of samples which are recognized mistakenly in the second sample set) / the total number of the second sample set.

(3) For total 742 test samples, 180 samples are rejected correctly and the other 2 samples are recognized mistakenly in the first test sample; and 536 samples are recognized correctly and the rest 24 samples are recognized mistakenly in the second test sample. Therefore, the rejection rate is 98.9% ($180/182$), the correct cognition rate and the error recognition rate are 95.71% ($536/560$) and 3.5% ($(2+24)/742$) respectively.

5. Experimental analysis

We can conclude from the above experimental results that:

(1) Irises are trained as "cognition" one class by one class in our method, and it doesn't influence the original recognition knowledge for samples of the new added class.

(2) Although the correct cognition rate is not very well, the result of rejection is wonderful. In our experiment, the rejection rate is 98.9%, namely, the iris classes that don't belong to the training test can be rejected successfully.

(3) The iris recognition algorithm based on neuron of multi-weighted neural network is applied in the experiment and the total samples of every class construct the shape of 1D distribution. Namely, it is the network connection of different neuron.

(4) The distribution of the recognized thing should be researched firstly when we apply the algorithm for iris recognition based on point covering theory of high-dimensional space. Then, the covering method of neural network is considered.

(5) In above experiment, if the image preprocessing is more perfectly, the experimental results maybe better.

To sum up, it proves the proposed iris recognition algorithm based on point covering of high-dimensional space and neural network is effective.

References

- [1] J.Daugman, Biometric Personal Identification System Based on Iris Analysis [P]. U.S. Patent 5291560, 1994.
- [2] J.Daugman, High Confidence Visual Recognition of Persons by a Text of Statistical Independence, IEEE Trans. Pattern Anal. Mach. Intell. 15(11) (1993) 1148-1161.
- [3] R.Wildes, Iris Recogniton: An Emerging Biometric Techonology, Proc. IEEE 85(1997) 1348-1363.
- [4] W.Boles, B. Boashash, A Human Identification Technique Using Image of the Iris and Wavelet Transform, IEEE Trans. Signal Process. 46(4) (1998) 1185-1188.
- [5] Wang Shoujue, Li Zhaozhou, Chen Xiangdong, Wang Bainan, Discussion on the Basic Mathematical Models of Neurons in General Purpose Neurocomputer, ACTA ELECTRONICA SINICA. 2001, 29(5): 577-580
- [6] Wang Shoujue, Xu Jian, Wang Xianbao, Qin Hong, Multi-camera Human-face Personal Identifications System Based on the Bionic Pattern Recognition, ACTA ELECTRONICA SINICA. 2003, 31(1): 1-3
- [7] Wang ShouJue, A New Development on ANN in China - Biomimetic Pattern Recognition and Multi weight Vector Neurons, LECTURE NOTES IN ARTIFICIAL INTELLIGENCE 2639: 35-43 2003
- [8] Yang Wen, Yu Li, et al, A Fast Iris Location Algorithm, Computer Engineering and Applications, 2004.10
- [9] Wang Yunhong, Zhu Yong, Tan Tieniu, Biometrics Personal Identification Based on Iris Pattern[J], ACTA AUTOMATICA SINICA, 2002. 28(1):1-10.
- [10] Li Ma et al. Local Intensity Variation Analysis for Iris Recognition, Pattern Recognition 37(2004) 1287-1298.
- [11] Han Fang, Chen Ying, Lu Hengli, An Effective Iris Location Algorithm, Journal of Shanghai University (Natural Science). 2001.7(6):01-03.
- [12] Wenming Cao, Feng Hao, Shoujue Wang: The application of DBF neural networks for object recognition. Inf. Sci. 160(1-4): 153-160 (2004)